

Modelling of integrated Peltier elements

D.D.L. Wijngaards, E. Cretu, S.H. Kong and R.F. Wolffenbuttel

Electronic Instrumentation Laboratory, Delft University of Technology / DIMES,
Department of Electrical Engineering, Mekelweg 4, NL-2628 CD Delft, The Netherlands
Phone: +31.15.278.1602, Fax: +31.15.278.5755, E-mail: d.d.l.wijngaards@its.tudelft.nl

ABSTRACT

On-chip integration of Peltier devices creates a number of additional parasitics, compared to conventional Peltier devices. The most important are thermal conduction through the supporting membrane and contact resistance. Analytical analysis shows that each parasitic decreases device performance, but only the contact resistance creates a significant shift in the optimum device current where the temperature reduction is maximised.

To obtain an energetically correct lumped-element model, as presented in this paper, the electro-thermal Peltier effect must be linked to the thermo-electric Seebeck effect, which acts as a feedback parameter. The influence of this Seebeck voltage on a non-ideal current source, driving the Peltier device, is investigated and it is shown that the influence can be ignored if the current source has a reasonable impedance.

Keywords: Peltier effect, on-chip cooling, thermoelectric refrigeration, thermal stabilisation, polySiGe

1 INTRODUCTION

The conventional Peltier device finds use in a range of applications, from thermal stabilisation [1,2] to micro refrigeration [3]. The operation of such devices has long been studied and is well documented in literature. An on-chip integrated counterpart could also be used for various applications, like fully integrated dew-point sensors, thermally stabilised optical detectors and radiation detectors or thermally stabilised on-chip references.

However, transformation of a conventional Peltier device, as schematically shown in Fig. 1a, into an integrated version, shown in Fig. 1b, is not straightforward. This paper addresses the consequences of this transformation, focusing on the practical behaviour of two major performance-limiting parameters, the parasitic thermal conduction through the supporting membrane and contact resistance. In the second part of this paper a new and simple lumped element model of a Peltier device is presented, which obeys the principle of conservation of energy. This model effectively links the temperature T_c of the thermally stabilised region to the ambient temperature T_a rather than to that of the heat sink temperature T_s . In Fig. 1b, T_s is the substrate temperature close to the Peltier element.

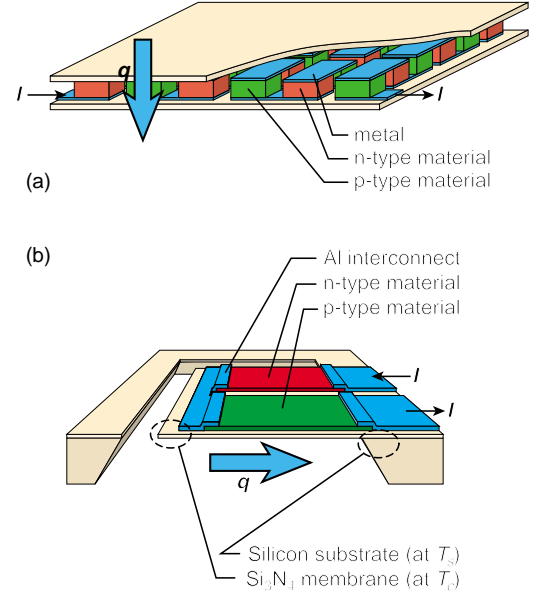


Figure 1: Schematic drawings of (a) a discrete Peltier device and (b) an integrated Peltier device.

2 ANALYTICAL MODEL

The behaviour of the conventional type of Peltier device, shown in Fig. 1a, is described by two simple equations, determining the heat transfer rate, q [W] and the maximum temperature reduction $\Delta T_{\max} = (T_s - T_c)_{\max}$:

$$q = (\alpha_p - \alpha_n) T_c I - K (T_s - T_c) - \frac{I^2 R}{2} \quad (1)$$

$$(T_s - T_c)_{\max} = \frac{(\alpha_p - \alpha_n)^2 T_c^2}{2 K R} = \frac{z T_c^2}{2} \quad (2)$$

The heat transfer rate is directly dependent on the parameters T_s , T_c and the electrical current I applied. Furthermore the heat transfer depends on the total thermal conductance, K , and the electrical resistance of the element, R , which consist of multiple parameters and are defined as

$$K = \frac{\lambda_n A_n}{L_n} + \frac{\lambda_p A_p}{L_p} \quad \text{and} \quad R = \frac{\rho_n L_n}{A_n} + \frac{\rho_p L_p}{A_p} \quad (3)$$

Parameters K and R incorporate the thermal conductivities λ , resistivities ρ , and geometrical parameters (cross-sectional area A and length L of the legs). The subscripts n and p indicate the n- and p-type legs of the device. Under the assumption of equations (1)-(3), ΔT_{max} is directly expressed as a function of the figure-of-merit z ($= \alpha^2/\lambda\rho$), and therefore is dependent on the material parameters of the device only. This simplifies the design of Peltier elements, as having determined the material parameters, the maximum temperature difference is fixed by (2), and can be obtained by selecting the proper device geometries as shown in [4]:

$$\frac{L_n A_p}{L_p A_n} = \left(\frac{\rho_p \lambda_n}{\rho_n \lambda_p} \right)^{1/2} \quad (4)$$

2.1 Integrated Peltier Device Model

Transformation of a conventional Peltier device into its integrated counterpart brings around three performance limiting factors. First, as a supporting membrane is required, parasitic thermal conductance through that membrane is introduced. Second, wafer processing strongly favours a device structure with Peltier elements in parallel with the membrane surface (as vertical stacking of multiple devices is costly and likely to reduce yield, although stacking might be necessary to increase the heat removal rate q). These two factors put an emphasis on low conductivity of the membrane, while it should also provide sufficient structural support. Third, contact resistance plays an increasingly important role with decreasing feature size, as is shown in the next section. When inserting all three limiting factors into (3), plus additional losses through radiation exchange and convection results in

$$K' = \underbrace{\frac{\lambda_n A_n}{L_n} + \frac{\lambda_p A_p}{L_p}}_K + \underbrace{\frac{\lambda_m A_m}{L_m} + \frac{\gamma A_r}{4}}_{K_{add}} = K + K_{add} \quad (5)$$

$$R' = \frac{\rho_n L_n}{A_n} + \frac{\rho_p L_p}{A_p} + 2R_{co} = R + 2R_{co} \quad (6)$$

The term λ_m indicates the thermal conduction through the membrane, while the fourth term in (5) combines the radiation losses and convection, while R_{co} indicates the contact resistance. Substituting (5) and (6) for (3) changes (2) to

$$(T_s - T_c)_{max} = \frac{(\alpha_p - \alpha_n)^2 T_c^2}{2 K' R'} = \frac{z T_c^2}{2 N}; \quad (7)$$

$$N = \left(1 + \frac{K_{add}}{K} + \frac{2R_{co}}{R} + \frac{2K_{add} R_{co}}{K R} \right) \quad (8)$$

Now ΔT_{max} , besides depending on z , also depends on the term N , including all geometrical parameters, which severely limits device optimisation. An excellent treatment of the integrated Peltier device model, which includes the influence of K_{add} , is presented by Völklein *et al.* in [5]. Nevertheless, the influence of contact resistance remains unaddressed.

2.2 Influence of the Contact Resistance

In this subsection, the influence by R_c on device performance is compared to the influence of λ_m . The influence by radiation exchange, has been estimated numerically to be less than 1% of the total heat transfer for small ΔT_{max} and will therefore be ignored. Furthermore, device operation in vacuum is assumed so convection can be ignored as well. As starting condition for the comparison, a Peltier device with polycrystalline SiGe (polySiGe) thermoelements is optimised according to (5), using the material parameters listed in Table 1 [4].

PolySiGe property	n-type	p-type
Seebeck Coefficient α [$\mu\text{V/K}$]	-136	144
Resistivity ρ [$\mu\Omega\text{m}$]	10.1	13.2
Conductivity λ [$\text{Wm}^{-1}\text{K}^{-1}$]	4.45	4.80
Figure-of-merit z [10^{-3}K^{-1}]	0.328	0.413
Doping concentr. [10^{20}cm^{-3}]	1-3	2-4

Table 1: Thermoelectric properties of polySiGe (from [4])

As heat transport in a Peltier device is controlled by the electrical current I applied, ΔT_{max} is plotted as a function of both I and the parasitic parameter of interest, either R_c or λ_m . The results are shown in Fig. 2. In both cases, the device performance decreases when either R_c or λ_m increase. However, unlike with λ_m , an increase of R_c does not only cause a decrease in device performance, but also causes a significant shift in the optimum device current I_{opt} as well. So, concluding from the analytical model, the effect of the contact resistance on device performance is a much larger source of concern than the effect of the thermal conduction through the membrane.

3 LUMPED-ELEMENT MODEL

The analytical model as described in the previous paragraph provides a very accurate solution for T_c with respect to the temperature reduction below the substrate temperature T_s . However, this model still has a number of shortcomings. First, it is energetically incorrect, and second, T_s is assumed equal to T_a , which on many occasions is false. The lumped-element model presented in this section addresses the energetical correctness, while the influence of the thermal conduction through the substrate, linking T_s to T_a is still under investigation.

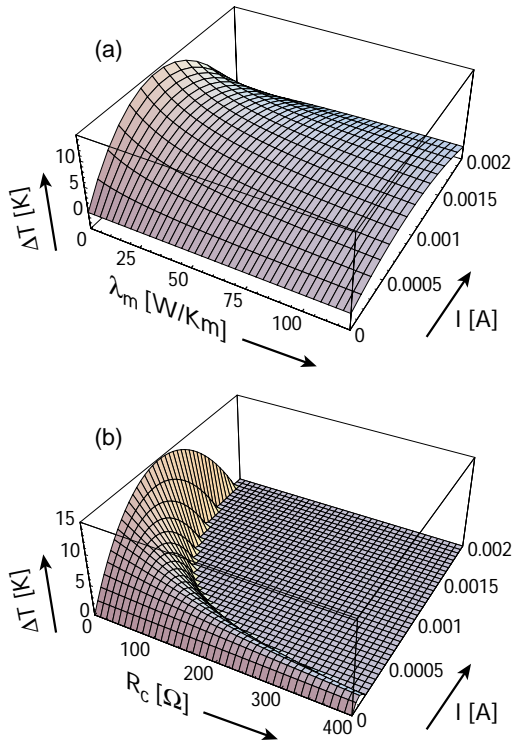


Figure 2: The influence on the maximum temperature reduction ΔT_{max} by (a) thermal conduction through the supporting membrane and (b) contact resistance.

An advantage of a lumped element analysis is that all parameters in the integrated Peltier device are modelled independently. Second, a lumped element analysis can provide a good estimation of the transient behaviour of the device. Most importantly, however, it is easy to implement cross-couplings, so an energetically correct model can be created, as will be shown.

3.1 Energetically correct model

The need for an energetically correct model of a Peltier devices should automatically arise when performing 3-D modelling. It is crucial that that such a system obeys the conservation of energy principle to obtain any meaningful result. In this respect, the Peltier effect behaves different

from Joule heating, as the former is a reversible effect. Consider the following reasoning: The rate of reversible energy absorption from the system at the cooled junction (at temperature T_c) is equal to $(\alpha_p - \alpha_n)T_c I$ and the rate of reversible energy released at the substrate (at temperature T_s) is equal to $(\alpha_p - \alpha_n)T_s I$. So, as T_c starts to drop with respect to T_s , more energy will be released than is absorbed, thereby violating the principle of conservation of energy. On the other hand, as the effect is reversible, changing the direction of the current flow implies that the amount of energy released is smaller then the amount absorbed. In either way, a violation of the principle of conservation of energy occurs. The solution to this inconsistency is simple, yet never used. When T_c drops with respect to T_s , the temperature difference $(T_s - T_c)$ results in a Seebeck emf e_{seeb} with value $((\alpha_p - \alpha_n)(T_s - T_c))$ [V]. The resulting power from this emf is equal to $e_{seeb} \cdot I$, which is exactly equal to the energy rate unbalance due to the Peltier effect. This way the reversible energy transfer complies with the principle of conservation of energy once more.

3.2 Thermoelectric Feedback

The previous paragraph proved that application of an electrical current to generate a temperature difference by the Peltier effect (electro-thermal energy conversion), also causes an electrical Seebeck voltage to appear (thermo-electrical energy conversion). Therefore, it is essential to combine both the Seebeck and Peltier effect in a single three-port element, as shown in Fig. 3.

The thermal and electrical domains in the model of Fig. 3 are connected by the three-port, and the three non-linear thermal energy sources on the right. As the energy generation in these sources is non-reversible, modelling as thermal energy sources rather than two-port elements is valid. On the left side of Fig. 3, the electrical current source I_g , with internal resistance R_g and equivalent load circuit R_l of the Peltier device is shown. The Joule heating q_j is distributed symmetrically over the capacitors $C_{th,c}$ and $C_{th,s}$, which represent the thermal capacity of the cooled area and the substrate. Furthermore, heat is generated by q_{co} due to contact resistance R_{co} . Finally, $R_{th,s}$ and $R_{th,c}$ indicate the thermal losses from the system to the ambient, on both the cooled side and the substrate side.

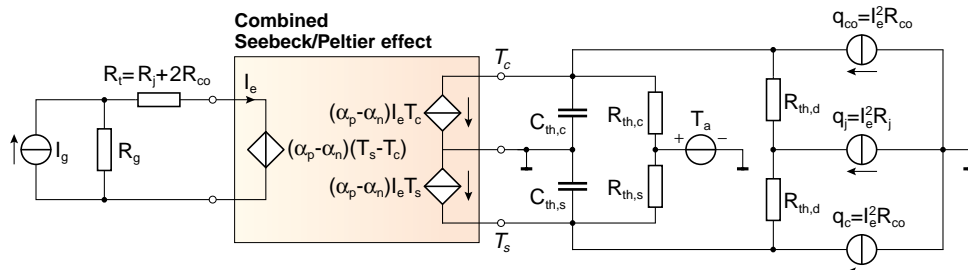


Figure 3: Thermoelectric lumped-element model of an integrated Peltier device, with a non-ideal electrical load, thermoelectric threeport element (including feedback), Joule heating effects and thermal distribution due to radiation, convection and conduction.

As the Seebeck emf is part of the current source's load, operation of the Peltier device influences the source current I_g due to the feedback. In this section, the influence by feedback is analysed, based on the lumped-element model of Fig. 3. As only the steady-state response is considered, $C_{th,c}$ and $C_{th,s}$ are ignored. Furthermore, the assumption is made that there is no radiation exchange or convection and that the substrate temperature is equal to the ambient temperature, e.g. $R_{th,s} = 0$ K/W and $R_{th,c} = \infty$. The remaining material parameters and geometrical parameters, next to those listed in table 1, are $L_p = L_n = L_m = 100$ μ m, $A_p = A_n = 30 \cdot 10^{-12}$ m², $A_m = 63 \cdot 10^{-12}$ m², $\lambda_m = 5$ W/mK and $R_{co} = 5$ Ω .

Inclusion or exclusion of the Seebeck effect in the lumped-element model does not influence ΔT_{max} , as this parameter is determined by the current I_e and not by I_g (shown by the dashed plots in Fig. 4b). However, as the Seebeck emf varies with ΔT , the current I_g will have to be compensated to maintain a constant I_e . To determine this influence by the Seebeck emf, the optimum current $I_{g,opt}$, where ΔT_{max} occurs (e.g. the curve describing the top of the curve in Fig. 4a) is calculated for two cases. In the first case, the Seebeck emf is ignored, while it is included in the second calculation. The difference is plotted as a function

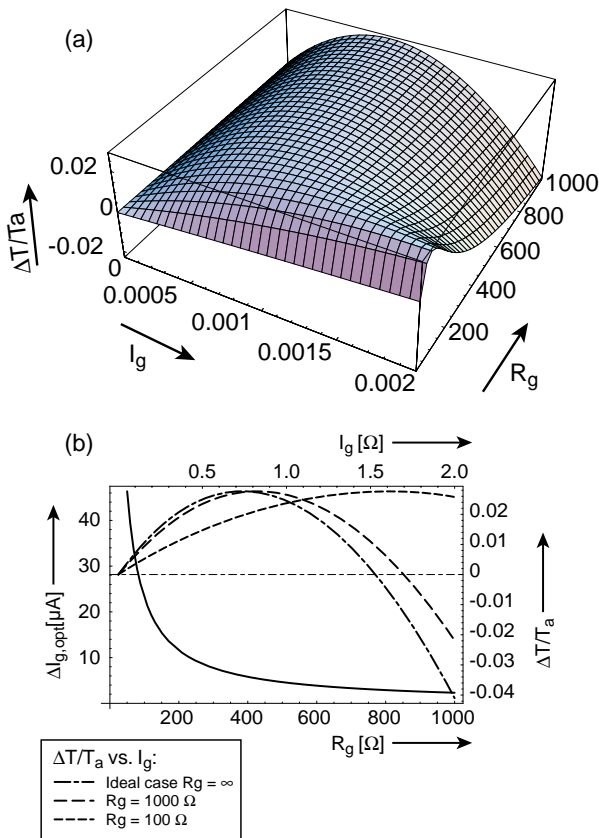


Figure 4: (a) A plot of the temperature reduction with respect to the source current I_g and source impedance R_g . (b) The shift in the optimizing source current I_g caused by the Seebeck effect, as a function of R_g .

of R_g in Fig. 4b. For very small values of R_g , (i.e. the current source is behaving rather like a voltage source) the required shift in I_g to maintain the right I_e is considerable. However, when driving the Peltier device with a well designed current source, the shift in I_g can be neglected. This implies that by using a properly designed driving circuit, the influence by the Seebeck effect may be ignored, even though this effect is required to obtain a correct energy balance.

4 SUMMARY AND CONCLUSIONS

On-chip integration of Peltier devices creates a number of parasitic effects, which are not present in the conventional type of device. The most important parasitics are thermal conduction through the supporting membrane and contact resistance. Comparison shows that an increase of each parasitic decreases device performance, but the contact resistance also results in a significant shift in the value of the current at which the maximum temperature reduction is obtained.

Compared to the conventional analytical analysis, the lumped-element model presented in this paper is energetically correct. Furthermore, the electro-thermal Peltier effect is linked to the thermo-electric Seebeck effect, thereby creating a feedback from the thermal to the electrical domain. The influence of this feedback on a non-ideal current source has been investigated and it is shown that the Seebeck emf (causing the feedback) may be ignored when using a current source with a reasonable internal impedance. Presently, extension of the model with losses due to radiation and convection, as well as conduction through the substrate, is investigated.

REFERENCES

- [1] A.W. Sloman, P. Buggs, J. Molloy and D. Stewart, A microcontroller-based driver to stabilize the temperature of an optical stage to within 1 mK in the range 4-38°C, using a Peltier heat pump and a thermistor sensor, Meas. Sci. Technol., vol. 7 no. 11 (1996) 1653-1664.
- [2] G. Festa and B. Neri, Thermally regulated low-noise, wideband, I/V converter, using Peltier heat pumps, IEEE trans. on IM, vol. 43 no. 6 (1994) 900-905.
- [3] M.R. Holman and S.J. Rowland, Design and development of a new cryosurgical instrument utilizing the Peltier thermoelectric effect, J. of Medical Engineering & Technology, vol. 21 no. 3-4 (1997) 106-110.
- [4] D.M. Rowe, CRC handbook of thermoelectrics, CRC Press, Boca Raton, Florida, USA, 1995.
- [5] F. Völklein, G. Min and D.M. Rowe, Modelling of a microelectromechanical thermoelectric cooler, Sensors and Actuators, A75 (1999) 95-101.